Leadership in Sustainable Infrastructure
Leadership en Infrastructures Durables

Vancouver, Canada
May 31 – June 3, 2017/ *Mai 31 – Juin 3, 2017*

SHORT CONCRETE COLUMNS REINFORCED WITH GFRP REBARS UNDER ECCENTERIC LOADING

Khorramian, Koosha[1], and Sadeghian, Pedram[1,2]
[1] Department of Civil and Resource Engineering, Dalhousie University, Canada
[2] Pedram.Sadeghian@dal.ca

Abstract: In this paper, the compressive performance of short concrete columns reinforced with glass fiber-reinforced polymer (GFRP) composite rebars is evaluated. A total of fourteen 500 mm long concrete specimens with square cross-section (150×150 mm) were prepared and tested under concentric and eccentric compressive loading up to failure. Nine of the specimens were reinforced with six GFRP rebars (16 mm diameter), longitudinally. Different eccentricities, namely, 0, 10, 20, and 30 percent of the width of the specimens were considered. Strain of GFRP rebars were monitored during the tests to evaluate the usable level of strain and mode of failure of rebars. It was observed that the GFRP rebars were able to withstand the peak concentric and eccentric loads without crushing and local buckling. It was concluded that the maximum usable strain of the GFRP rebars in compression was larger than the ultimate compressive strain of concrete, 0.0035, defined by CSA A23.3 and the compressive contribution of GFRP rebars in column capacity is not negligible. This is an ongoing research and more results regarding compressive behavior of GFRP rebars and their contribution to the axial-bending interaction diagram will be presented at the time of the conference.

1 INTRODUCTION

Glass fiber-reinforced polymer (GFRP) rebars have been used as an alternative to steel in concrete because of their resistance to corrosion, low electrical conductivity, high strength to weight ratio, and a lower maintenance cost (Benmokrane et al. 1995). To design concrete columns reinforced with GFRP rebars, many researchers were involved. For example, under combined axial and flexural loads researchers tried to develop similar methods to the design of steel columns by finding strength reduction factor for GFRP rebar reinforced concrete (Zadeh et al. 2013, Mirmiran et al. 2013). In addition, parametric studies on GFRP under eccentric loading, configuration, tie spacing, spalling of concrete cover, reveals that GFRP rebar can withstand loads similar or higher than steel (Tobbi et al. 2012). Other researchers tried to assess the behavior of slender high strength concrete reinforced with GFRP rebar under eccentric and concentric loading (Hales et al. 2016). Other researchers worked on the interaction diagrams of GFRP bar reinforced concrete columns (Karim et al. 2016). These efforts aimed to improve the design of concrete columns reinforced by FRP rebars. However, there are still some gapes in assessing the behavior of these columns.

It is believed that the compression strength of GFRP rebars in compression is not comparable to its strength in tension. For example, the ACI design guide for GFRP rebars (ACI 440.1R 2015) neglects the contribution of the GFRP rebar in compression. Another example is Canadian standard for design and construction of building structures with GFRP (CAN/CSA S806-12. 2012) which allows the use of GFRP rebars in concentrically loaded columns only if the designer neglects their contribution in strength. On the other hand, an experimental study by Tobi et al. (2012), showed 35 percent contribution of GFRP rebar in the load

carrying capacity of concentrically loaded columns by comparing their results to previous suggested formulas by researchers as presented in equation 1 (Tobbi et al. 2012).

[1] $$P_n = 0.85\, f'_c (A_g - A_f) + 0.35\, f_{ftu} A_f$$

In equation 1, P_n is the ultimate capacity of a GFRP reinforced concrete column, f'_c is the compressive strength of concrete, A_g is the gross cross sectional area, A_f is the GFRP cross sectional area, and f_{ftu} is the ultimate tensile strength of GFRP rebar. Although researchers have tried to show the contribution of the FRP rebar in compression, building codes and specifications still do not allow the designer to take the compressive strength of GFRP into account due to lack of proving data and experimental work. On the other hand, the behavior of concrete columns under eccentric loading could reveal GFRP contribution in compression for the case of combined compressive and flexural loading in order of comparison. Thus, in this paper, the behavior of short concrete columns reinforced with GFRP rebars under both pure axial and combined axial load and bending moment as well as the GFRP functionality in compression are studied. The main focus of this study is to figure it out how much compressive strain can a GFRP rebar sustain under compression loading without crushing or buckling.

2 EXPERIMENTAL PROGRAM

2.1 Test Matrix

A total of fourteen 500 mm long concrete columns with a square cross section (150×150 mm) were tested under pure uniaxial compressive as well as combined axial and flexural loads. Nine of these specimens were reinforced with six GFRP bars. Four specimens consisting two plain concrete and two concrete columns reinforced with GFRP were tested under pure axial load and other specimens were tested under eccentric loads of 10, 20, and 30 percent of width of the cross section. To name the specimens, a label like “A-ex-y” is used where x, y, and C are the column type, the eccentricity, and the specimen number, respectively. The column type is identified by “P” for plain, or “R” for rebar reinforced concrete columns. For example, “R-e10-2” means that the column was the second specimen that was tested under 10 percent of width eccentricity and reinforced with rebar. The test matrix is provided in Table 1.

Table 1. Test Specimen Properties

No.	Specimen ID	Eccentricity (mm)	Reinforcement
1	R-e0-1	0	GFRP
2	R-e0-2	0	GFRP
3	R-e10-1	15	GFRP
4	R-e10-2	15	GFRP
5	R-e10-3	15	GFRP
6	R-e20-1	30	GFRP
7	R-e20-2	30	GFRP
8	R-e30-1	45	GFRP
9	R-e30-2	45	GFRP
10	P-e0-1	0	Plain
11	P-e0-2	0	Plain
12	P-e10-1	15	Plain
13	P-e10-2	15	Plain
14	P-e10-3	15	Plain

2.2 Material Properties

To reinforce the concrete columns, six #5 GFRP rebars with a diameter of 16 mm and nominal cross-sectional area of 197.9 mm^2 were used in this study. To determine tensile characteristics of rebars, five tensile specimens were tested per ASTM D7205M (ASTM D7205M 2011). The tensile strength, tensile modulus, and ultimate tensile strain of rebars were evaluated as 629±30 MPa, 38.7±1.5 GPa, and 0.0162±0.0011 mm/mm, respectively. The concrete strength at the time of testing was recorded as 37 MPa by testing three concrete cylinders (100×200 mm).

2.3 Fabrication

The concrete was casted in wooden molds which had been prepared to hold the rebars. The movement of rebar was restricted by two rigid wooden plates with holes that were attached to the top and bottom of the column. Th cover of GFRP rebar was selected as 25.4 mm in each direction which is consistent with available specifications for fiber-reinforced polymer rebar (ACI 440.1R 2015). The center to center distance between two rebars was 41.6 mm, and the distance from the edge of concrete to the center of rebar was 33.4 mm. There were two rows of rebar that each of them consisted of three rebar as is shown in Fig 1.

Since the load concentration at bottom and top of the specimens, where the load applied, was expected to cause a premature failure, both ends of concrete columns were strengthened with Basalt wraps. Two layers of 50 mm wide unidirectional Basalt fabrics were installed using epoxy resin. Then, the top and bottom surfaces were flattened by means of a grinder to remove extensions of rebar and wrapped parts and to provide a smooth surface at top and bottom of each specimen.

2.4 Test Set-up

The desired boundary condition and load eccentricity in these column tests were fulfilled using two steel caps at top and bottom of each specimen. The steel cap consists of a notched, 30 mm thick steel plate welded on a rigid steel plate (250×250×10 mm). To satisfy the pin-pin boundary condition, two steel cylinders, as shown in Fig 1, were put on the notch while their other side was fixed to the testing machine. The function of cylinder and notched plate was to make the rotation happen at both ends of the column. There was some grease on the interface of notched plate and cylinder for lubrication. Moreover, four adjustable angle profiles were nailed to the plate to force the column rotate consistently with the steel cap.

Since both concrete columns and steel caps were solid, plastic bags filled with fresh grout were used at the time of assembling so that its plastic nature cover the gaps between their interface and integrate them when the grout was set. In addition, the load eccentricity changed by moving the notched plate on the rigid steel plate and fixing it by weld. All eccentrically loaded specimens were tested under single curvature condition where the eccentricity at both ends were the same.

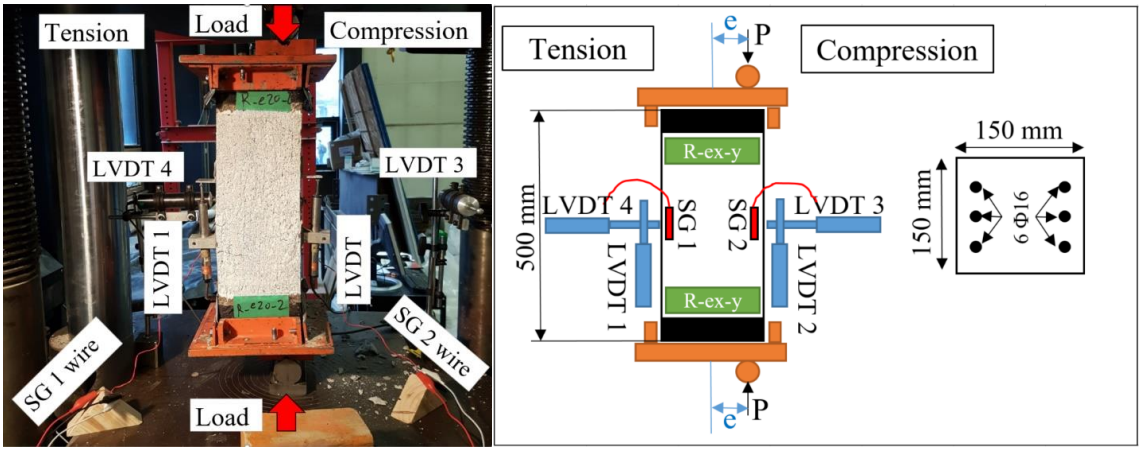

Fig 1. Test set up and instrumentation

To analyze the behavior of the specimens, the strains and displacement were measured by means of a data acquisition system reading the data from strain gauges and LVDTs at 0.1 sec time steps. The schematic test set up is shown in Fig 1. The strain gauges on two central rebars in compression and tension side of eccentrically loaded specimens measured the longitudinal strains at the outer side of the rebar. Meanwhile, a system of LVDTs and angles with a gauge length of 100 mm were attached to both sides of the concrete to verify the strain of the rebars using the linear strain variation assumption. Furthermore, two horizontally LVDTs were aligned with the center of concrete columns to measure the deflection of the mid span. The load and stroke were read from the testing machine directly. The test was performed by a 2MN universal testing machine with a displacement control approach and a rate of 0.625 mm/min.

3 RESULTS AND DISCUSSION

The test results including the peak load, maximum recorded strain values and its ratio to the reported ultimate tensile strain for both tension and compression sides, the strain at which the peak load dropped by 15 percent, and the modes of failure are presented in Table 2.

Table 2. Summary of test results

No.	Specimen ID	Peak Load (kN)	Maximum strain SG1 (mm/mm)	SG1 to rupture strain ratio	SG1 @ 0.85 peak (mm/mm)	Maximum strain SG2 (mm/mm)	SG2 to rupture strain ratio	SG2 @ 0.85 peak (mm/mm)	Failure mode
1	R-e0-1	774.9	-0.00541	0.33	-0.00527	-0.00535	0.33	-0.00459	CC → CS
2	R-e0-2	451.6	-0.00113	0.07	-	-0.00076	0.05	-	LS
3	R-e10-1	692.3	-0.00064	0.04	-0.00012	-0.00451	0.28	-0.00323	CS & LS
4	R-e10-2	507.0	-0.00057	0.04	-	-0.00656	0.40	-0.00376	LS
5	R-e10-3	693.3	0.00293	0.18	-0.00017	-0.00555	0.34	-0.00509	CC → CS
6	R-e20-1	589.6	0.00206	0.13	0.00053	-0.00824	0.51	-0.00639	CC → CS
7	R-e20-2	566.7	0.00220	0.14	0.00048	-0.00327	0.20	-0.00305	CS → ST
8	R-e30-1	363.6	0.00144	0.09	0.00139	-0.00906	0.56	-0.00650	CC → CS
9	R-e30-2	344.6	0.00294	0.18	0.00277	-0.00709	0.44	-0.00525	CC → CS
10	P-e0-1	791.0	-	-	-	-	-	-	CS
11	P-e0-2	647.4	-	-	-	-	-	-	CS
12	P-e10-1	589.1	-	-	-	-	-	-	CS → CD
13	P-e10-2	509.3	-	-	-	-	-	-	CS → CD
14	P-e10-3	690.5	-	-	-	-	-	-	CS → LS

Note: The positive and negative signs assigned to tensile and compression strains, respectively.

The strain diagrams read from strain gauges are presented in Fig 2 through Fig 4, and the broken GFRP reinforced specimens are shown in Fig 5. It is observed that in both pure compressive and combined compressive and flexural loading, the GFRP reinforced concrete specimens sustained more load than plain specimens.

As it is shown in Fig 2 through Fig 4, all reinforced specimens experienced considerably larger strains than the tensile strain gauges. Fig 4 shows that as the eccentricity increases, the peak load decreases and the strains tends to be larger for reinforced specimens. The lateral displacement at peak load and the slope of ascending branch of lateral load-displacement graph remains similar for 10 and 20 percent eccentricity ratios while it tends to be stretched for 30 percent eccentricity ratio which means lower stiffness expectation by increasing the eccentricity. The ultimate displacement, on the other hand, tends to be lower as the eccentricity increases that shows the lower axial load and bending moment sustainability of higher eccentrically loaded specimens.

The ultimate strains of specimens were considered as the strain at which the axial load was dropped 15 percent according a study on combined axial and flexural loads performed by Hognestad (Hognestad 1951). Four modes of failure were detected as shown in Table 2, including concrete crushing in compression (CC), concrete spalling in compression (CS), concrete destruction (CD), and longitudinal splitting (LS). However, buckling or crushing of GFRP rebars were not observed. The concrete crushing (CC) is defined as the state at which the strain in the interface of rebar and concrete, after 15 percent drop of peak load, reaches 0.0035 (CSA A23.3, 2014). The separation of concrete segments from the column defined as concrete spalling (CS).

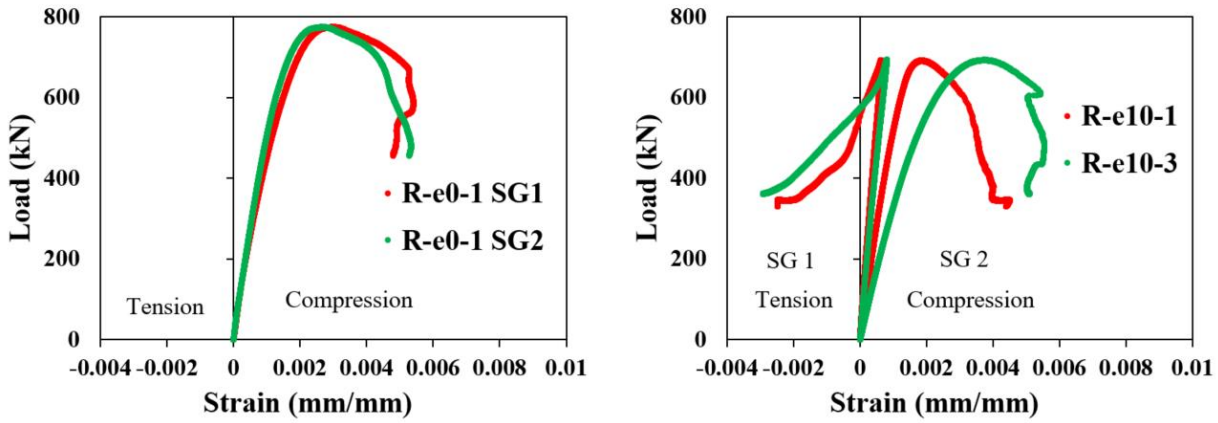

Fig 2. Compression and tension strain gauges for 0 and 10 percent eccentricity ratio

For 10 percent eccentricity ratio, the plain concrete specimens suddenly exploded at peak load and split in half, P-e10 specimens in Table 2. Nearly all reinforced concrete specimens experienced a crushing in compression side of the concrete columns and then spalled. There were two longitudinally cracked specimens, R-e0-2 and R-e10-2 that were lost their strength suddenly and just after the appearance of the cracks. The latter states identified as the premature failure in the column and the corresponding specimens considered as test failure. In addition, R-e20-2 specimen was stopped by the operator because of being suspicious about destructive consequences of explosion of concrete.

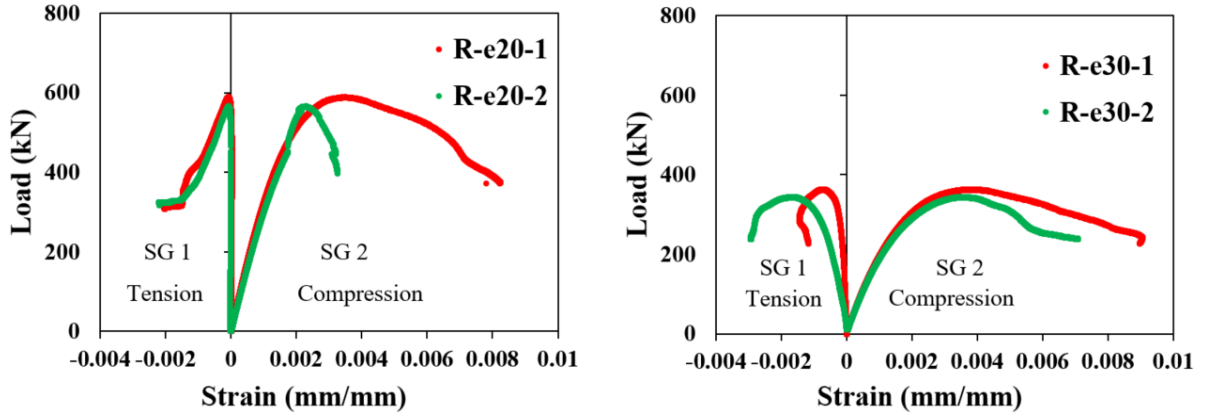

Fig 3. Compression and tension strain gauges for 20 and 30 percent eccentricity ratio

As it is plotted in Fig 3, for R-e20-2, the strain in compressive rebar has not been continued as the load dropped while the strain in tensile side is continued. This could be due to the separation of the strain gauge from the rebar in compression side. Due to the noises in the ascending branch there could be a possibility of partial separation of strain gauge from the rebar even before reaching the peak load, and that could be

the reason why the compressive strain part of R-e20-2 is shorter than the values read for R-e20-1. It is observed that both at peak load and after that, the strain in compressive rebar were higher in comparison with the strain in tension side. The ratio of the ultimate strain in GFRP rebar in compression side (SG2) to the tensile rupture strain of GFRP bars (0.0162 mm/mm) are presented in Table 2. The average ratios of R-e10, R-e20, and R-e30 without crushing or buckling of GFRP rebar, neglecting R-e10-2, are 0.310, 0.355, and 0.498 (average ratio =0.388) while this ratio for tensile rebar are 0.110, 0.131, and 0.135 (average ratio =0.126).

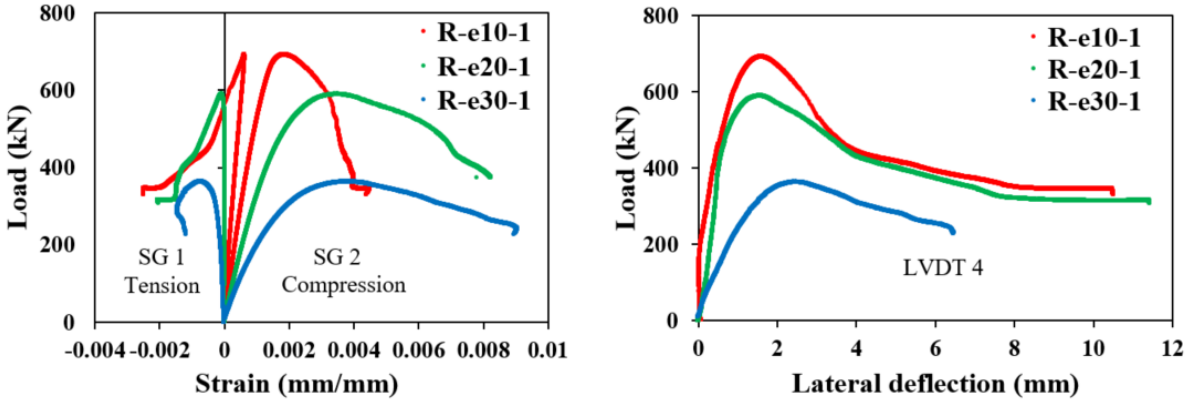

Fig 4. Load vs strain and lateral of GFRP specimens

In this study, GFRP rebars tolerated 39% of their tensile strain rupture, averagely. Majority of compressive rebars in specimens experienced compressive strains more than 0.0035 mm/mm without being buckled or crushed at 85 percent drop point after the peak load. In other words, GFRP rebar sustain compressive loads even after crushing of concrete. Overall, the results show that the contribution of GFRP in column capacity is not negligible and has more effects in higher eccentricities.

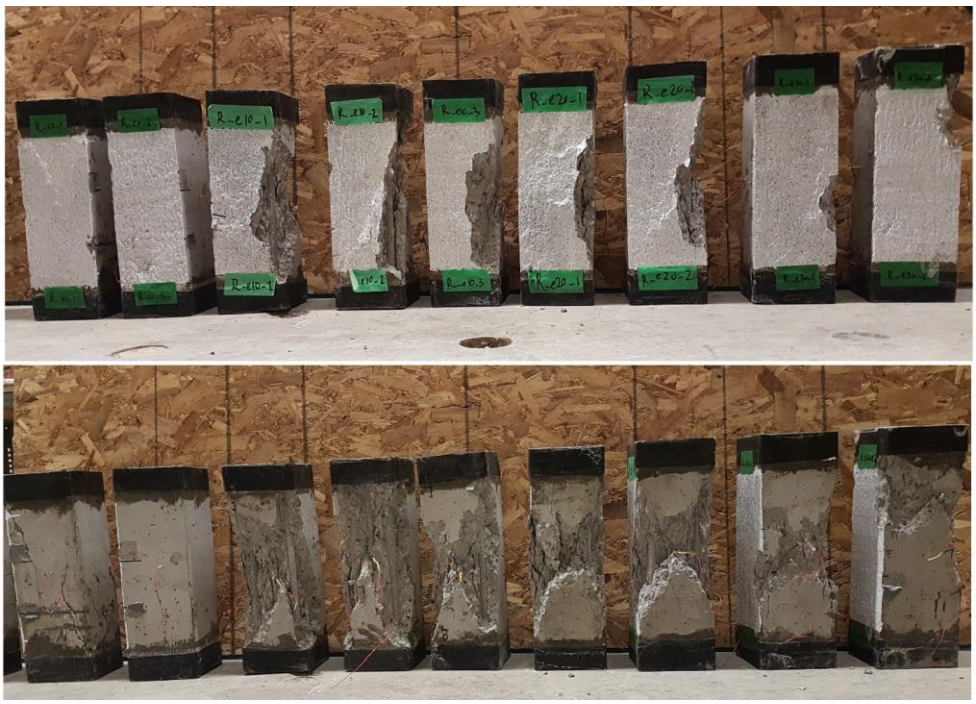

Fig 5. GFRP reinforced specimens after failure

4 CONCLUSION

This study tried to investigate the performance of GFRP rebars in compression in short concrete columns by means of performing an experimental program including fourteen GFRP reinforced and plain concrete columns eccentrically loaded up to failure. It was observed that compressive rebars tolerate the load without buckling or crushing while the concrete columns experienced concrete crushing, concrete spalling, longitudinally splitting in half and, complete destruction modes of failure. The contribution of rebars in compression was 39 percent of the tensile rupture strain of rebar which is determined by material test. Due to the fact that the recorded strain in compressive rebars exceeds the defined crushing strain of concrete in compression (0.0035 mm/mm), it is concluded that the rebars in compression contribute to the column capacity even after concrete crushed.

4 ACKNOWLEDGEMENT

The authors are grateful for the financial support of the Natural Sciences and Engineering Research Council of Canada (NSERC) in conducting this study.

5 REFERENCES

ACI 440.1R. 2015. Guide for the Design and Construction of Structural Concrete Reinforced Fiber-Reinforced Polymer (FRP) Bars, American Concrete Institute.

ASTM D7205M-06R11. 2011. Standard Test Method for Tensile Properties of Fiber Reinforced Polymer Matrix Composite Bars, American Society of Testing and Material.

Benmokrane, B., Chaallal, O. and Masmoudi, R. 1995. Glass fibre reinforced plastic (GFRP) rebars for concrete structures. Construction and Building Materials, 9 (6): 353-364.

CAN/CSA A23.3. 2014. Design of concrete structures, Canadian Standard Association.

CAN/CSA S806-12. 2012. Design and Construction of Building Structures with Fibre-Reinforced Polymers. Canadian Standards Association.

Hales, T.A., Pantelides, C.P. and Reaveley, L.D. 2016. Experimental Evaluation of Slender High-Strength Concrete Columns with GFRP and Hybrid Reinforcement. Journal of Composites for Construction, 04016050.

Hognestad, E. 1951. *A Study of Combined Bending and Axial Load in Reinforced Concrete Members,* University of Illinois Bulletin, Urbana, Illinois, USA.

Karim, H., Sheikh, M.N. and Hadi, M.N.S. 2016. Load and Moment Interaction Diagram for Circular Concrete Columns Reinforced with GFRP Bars and GFRP Helices. *Journal of Composites for Construction*, 04016076.

Mirmiran, A., Yuan, W. and Chen, X. 2001. Design of Slenderness in Concrete Columns Internally Reinforced with Fiber-Reinforced Polymer Bars. *ACI Structural Journal*, 98 (1): 116-125.

Tobbi, H., Farghaly, A.S. and Benmokrane, B. 2012. Concrete Columns Reinforced Longitudinally and Transversally with Glass Fiber-Reinforced Polymer Bars. *ACI Structural Journal*, 109 (4): 551-558.

Zadeh, H.J. and Nani, A. 2013. Design of RC columns Using Glass FRP Reinforcement. *Journal of Composites for Construction*, 17 (3): 294-304.